THE JOURNAL OF COMPARATIVE NEUROLOGY 373:41-54 (1996)

Structure, Development, and Maintenance of the Nerve Net of the Body Column in Hydra

M. SAKAGUCHI, A. MIZUSINA, AND Y. KOBAYAKAWA
Department of Biology, Faculty of Education, Shinshu University, Nishinagano, Nagano 380 Japan (M.S., A.M.); and Department of Biology, Faculty of Science, Kyushu University, Roppon-matsu, Fukuoka 810 Japan (Y.K.)

ABSTRACT

The anatomy and developmental dynamics of the nerve net in the body column of *Hydra viridissima* were examined immunocytochemically with a monoclonal antibody (CC04) that recognizes an antigen in nerve cells and with an antiserum against vasopressin. $CC04^+$ neuron cell bodies, their neurites, and vasopressin-like-immunoreactive (VLI^+) neurites could be clearly visualized on whole-mount preparations. All neurites of the $CC04^+$ neurons in the body column were VLI^+. However, only half of the VLI^+ neurites in the body column were $CC04^+$. Immunocytochemical analysis of macerated preparations showed that half of the neurons in the gastric region of the body column were $CC04^+$. These results suggest that most of the neurons in the gastric region are VLI^+. The density of the VLI^+ neurites was uniform along the entire length of the body column. The $CC04^+$ neuron density in the gastric region remained constant at all stages of asexual development and during foot regeneration. After pulse-labeling with 5-bromo-2'-deoxyuridine (BrdU), $CC04^+$ neurons with labeled nuclei appeared in the body column. We conclude that neuron density in the gastric region is maintained at a constant value by insertion of new neurons in parallel with continuous epithelial cell division.

Indexing terms: immunocytochemistry, vasopressin, monoclonal antibody, neuron, density

Understanding the formation, maintenance, and plasticity of neural networks is a central problem in developmental neurobiology. Hydra, a freshwater cnidarian, has provided a simple and unique model system for investigation of these questions (Bode, 1988; Bode et al., 1988).

Hydra has a very simple nervous system consisting of a nerve net that extends throughout the animal's body (Hadzi, 1909; Burnett and Diehl, 1964; Lentz and Barrnett, 1965). The body of hydra is basically a tube with a head at one end, and a foot at the other end. The body consists of two epithelial layers, the ectoderm and endoderm, separated by the mesoglea, a basement membrane. The cell bodies of neurons are found mostly near the basal sides of the two epithelial cell layers. The neurites are intertwined among the epithelial cells.

Hydra neurons can be divided into two classes on a morphological basis: ganglion cells and sensory cells (Westfall, 1973; Westfall and Kinnamon, 1978; Bode et al., 1988; Koizumi et al., 1988). Using antisera against neuropeptides and monoclonal antibodies against unknown antigens, it has been found that the nervous system of Hydra consists of many subsets of neurons (Grimmelikhuijzen et al., 1980, 1981a–c, 1982a,b; Grimmelikhuijzen, 1983; Dunne et al., 1985; Koizumi and Bode, 1986, 1991; Yaross et al., 1986; Koizumi et al., 1988, 1992; Hobmayer et al., 1990a,b).

In the body column of hydra, the epithelial cells are continuously undergoing cell division (Campbell, 1967a; David and Campbell, 1972; Holstein et al., 1991). Although the epithelial tissue is continuously growing, the size of an adult animal remains constant. This constancy in size arises as a result of the fact that the epithelial cells are continuously displaced towards the extremities, where cells are lost by sloughing, or into developing buds which eventually detach (Campbell, 1967b; Otto and Campbell, 1977b). Because the nerve net is intertwined among the epithelial cells, individual neurons continually change their location within the animal in a coordinated fashion with epithelial tissue movement (Yaross et al., 1986). The neurons are eventually lost at the extremities as is the case with the epithelial cells. Despite this constant tissue displacement, the distributions of individual subsets of neurons, which are defined by staining with various antibodies, are maintained.

Accepted April 11, 1996.

Address reprint requests to Dr. Masahiko Sakaguchi, Department of Biology, Faculty of Education, Shinshu University, Nishinagano, Nagano 380, Japan. E-mail: BIOLOGY@GIPNC.SHINSHU-U.AC.JP

As Bode (1988) has pointed out, with epithelial cells of the body column continuously dividing, the "mesh size" of the associated nerve net should continuously increase and neuron density should decrease if new neurons are not inserted into the preexisting nerve net. However, new neurons arise continuously by differentiation from interstitial cells (David and Murphy, 1977) and are added to the body column (David and Gierer, 1974). As a result of this addition of new neurons, the number of neurons per ectodermal epitheliomuscular cell remains constant in the gastric region (Bode et al., 1973). These results suggest that newly differentiated neurons are inserted into the net in a manner which is coordinated with the process of epithelial cell division. However, the precise spatial organization of the nerve net in the hydra body column is poorly understood, and it remains to be elucidated how new neurons are inserted into the preexisting nerve net of the body column. Here, we report the structure and developmental dynamics of the nerve net in the body column as visualized by a monoclonal antibody, termed CC04, and an antiserum against the neuropeptide vasopressin.

MATERIALS AND METHODS

Hydra strains and culture

The L9 strain of *Hydra viridissima,* which harbors numerous symbiotic algae in the endodermal cells, has been maintained by Dr. T. Sugiyama (National Institute of Genetics, Japan) since 1988. This strain was originally collected in northern California in 1987 by Drs. C. Teragawa and L. Littlefield. An algae-free version of this strain was prepared by Dr. Sugiyama using treatment with 50 μg/ml refampicin and 50 μg/ml kanamycin in modified M solution (Takano and Sugiyama, 1983) in constant darkness. The progeny of this algae-free strain has been maintained since 1990 in our laboratories as strain 55. Strain 55 was used in all experiments because of the absence of autofluorescence from the symbiotic algae. Animals were cultured in modified M solution containing 0.02 mM EDTA (hydra medium) at 19 ± 1°C, with a 12-hour light-dark cycle. Animals were fed with brine shrimp larvae daily except Sunday, and rinsed twice at 2 hours and 6 hours after feeding. All animals were starved for 1 day before fixation for immunocytochemistry.

Definition of body regions

There has been some variation in the use of the term "body column" among investigators working with hydra (e.g., Bode et al., 1973; Campbell and Bode, 1983; Koizumi and Bode, 1986; Holstein et al., 1991). In this paper, head refers to the region consisting of the hypostome, the tentacle base, and the tentacles. Foot refers to the basal disk. The remainder of the animal, consisting of the gastric region and the peduncle, is referred to as the body column. The gastric region includes the budding zone. The peduncle consists of the tissue proximal to the budding zone and distal to the basal disk.

Antibodies

Monoclonal antibodies were raised as described by Dunne et al. (1985). Briefly, a 6-week-old BALB/c female mouse was innoculated intraperitoneally with a few hundred hydra polyps of the species *Pelmatohydra robsta,* which had been homogenized by sonication in phosphate-buffered saline (PBS; 0.15 M NaCl, 0.01 M phosphate buffer, pH 7.2). Four weeks later, the mouse received a second intraperitoneal injection of hydra homogenate. Three days later, the spleen was removed and fused with cells of the P3U1 mouse myeloma line. Colonies which survived culture in hypoxanthine/aminopterin/thymidine medium were isolated and screened by immunocytochemistry as described below. We obtained a monoclonal antibody, termed CC04, in this process. This antibody is of the immunoglobulin G class (IgG).

The rabbit anti-vasopressin antiserum was purchased from Immuno Nuclear Corp. (USA) and kindly provided by Dr. O. Koizumi (Fukuoka Women's University, Japan).

Immunocytochemistry on whole-mount preparations

All steps for immunocytochemistry were done at room temperature unless otherwise indicated. Animals were anesthetized in 2% urethane (Sigma, St. Louis, MO) in hydra medium for 1 minute. For staining with the CC04 antibody, the relaxed polyps were fixed with methanol for 1 hour and then washed in PBS plus 0.05% Tween 20 (PBST) for 30 minutes. Next, the animals were incubated in PBS containing 1% skim milk (Yukijirusi Milk Corp., Japan) for 1 hour followed by incubation for 2 hours with culture supernatant from the hybridoma which produces the CC04 antibody. After a PBST wash, polyps were incubated with fluorescein isothiocyanate (FITC)-conjugated goat anti-mouse IgG (Vector, USA; 1:200 dilution in PBS containing 0.5% bovine serum albumin (BSA) and 0.1% NaN_3) for 2 hours. Finally, the animals were washed in PBST, and mounted in PBS-glycerol (1:3).

For double staining with the CC04 antibody and anti-vasopressin antiserum, the relaxed polyps were fixed with 10% formalin in PBS for 1 hour. After washing with PBST, the animals were incubated in 0.4 M glycine for 30 minutes and washed with PBS containing 0.25% Triton X-100 (PBS-Triton) for 30 minutes. After incubation in PBS-Triton containing 1% skim milk for 1 hour, the animals were incubated with the CC04 antibody (culture supernatant) for 2 hours. After a PBS-Triton wash, polyps were incubated with Texas Red-conjugated goat anti-mouse IgG (Vector; 1:200 dilution in PBS-Triton containing 0.5% BSA and 0.1% NaN_3) overnight at 4°C. After a PBS-Triton wash, the animals were incubated in anti-vasopressin antiserum (1:500 dilution) for 2 hours. After a PBS-Triton wash, polyps were incubated with FITC-conjugated goat anti-rabbit IgG (Vector; 1:200 dilution) for 2 hours. Finally, the animals were washed with PBS-Triton and mounted in PBS-glycerol. Immunofluorescence was detected by a Nikon fluorescence microscope fitted with filters selective for fluorescein (B: EX450–490; DM505; 460; 515W) and Texas Red (G: EX 546/10; DM575; 580W). As a negative control, either CC04 antibody or anti-vasopressin antiserum was omitted; no cross-reactivity was detected when the incubations were done sequentially as indicated.

For staining with the anti-vasopressin antiserum alone, the steps for the CC04 antibody described above were omitted. To be sure that the antiserum recognized vasopressin or a related molecule, the antiserum was preincubated overnight with 1, 10, or 100 μg of vasopressin and then subsequently used to stain whole-mounts. At all three concentrations, staining was abolished.

Immunocytochemistry on cells from macerated polyps

The gastric region was excised from polyps with a single bud at stages 8–10. The bud stages are the same as those described for *H. attenuata* (now called *H. vulgaris*) by Otto and Campbell (1977a). First, the peduncle and basal disk, which is just proximal to the bud protrusion, and the head were removed by amputation. The bud was then removed, leaving the gastric region. The gastric regions from ten animals were macerated in 100 μl of glacial acetic acid, glycerol, and water (1:1:13) in a polystyrene tube as described by David (1973). After addition of 100 μl of 10% formalin, 20 μl of the solution was spread on a gelatin-coated slide. The slides were dried for 1 hour at 60°C, postfixed with 10% formalin in PBS for 30 minutes, and washed for 10 minutes in PBST. The slides were incubated in the following sequence of solutions: 1% skim milk in PBS for 30 minutes; the CC04 antibody (culture supernatant) for 2 hours; PBST for 10 minutes; alkaline-phosphatase-conjugated goat anti-mouse IgG (Vector; 1:200 dilution in PBS containing 0.5% BSA and 0.1% NaN_3) for 1 hour; PBST for 10 minutes. Alkaline-phosphatase was detected by incubating the slides for 10 minutes in 0.1 M Tris, 5 mM $MgCl_2$, 0.1 M NaCl, pH 9.5 containing 0.17 mg/ml 5-bromo-4-chloro-3-indolylphosphate p-toluidine salt (BCIP, Sigma) and 0.33 mg/ml nitro blue tetrazolium (NBT, Sigma). The slides were washed in distilled water, followed by addition of PBS-glycerol and a coverslip over the cells. Each cell type on the slides was counted using a Nikon microscope with interference contrast optics.

BrdU pulse-labeling and double staining with anti-BrdU antibody and CC04 antibody on whole-mount preparations

Labeling with the thymidine analog 5-bromo-2′-deoxyuridine (BrdU) was done according to the procedures described previously (Teragawa and Bode, 1990; Holstein et al., 1991; Koizumi et al., 1992). Polyps were labeled with BrdU (Sigma) by introducing into the gastric cavity with a polyethylene needle an aqueous solution of 1.0 or 5.0 mM BrdU in hydra medium. The animals were then incubated with 1.0 or 5.0 mM BrdU in hydra medium for 1 hour at 19°C, washed, and cultured in hydra medium. The labeled animals were fed daily until two days before fixation. At the time of analysis, the animals were relaxed with 2% urethane in hydra medium, then fixed with 75% ethanol for 1 hour. After washing with PBST, the animals were incubated in PBS for 30 minutes at 80°C. After washing with distilled water, animals were incubated in 2 N HCl for 30 minutes. After a PBST wash, animals were incubated in PBS containing 1% skim milk for 1 hour followed by incubation with an anti-BrdU monoclonal antibody (Boehringer Mannheim; 1:20 dilution in PBS containing 0.5% BSA and 0.1% NaN_3) for 2 hours. After a PBST wash, the animals were incubated with Texas Red-conjugated goat anti-mouse IgG (Vector; 1:200 dilution) for 2 hours. The animals were then washed twice in PBST and incubated in fresh PBST overnight at 4°C. Then they were incubated in PBS containing 1% skim milk for 1 hour. Next, the animals were incubated with the CC04 antibody and FITC-conjugated goat anti-mouse IgG as described above.

Quantification of the neuron density in whole-mount preparations

Immunoreactive neurons in all regions of the animals on whole-mounts were photographed. Only the stained neurons on the half of the animal facing the objective could be clearly visualized in a single focal plane. From combined photographs, the neurons were traced on transparent film to allow the spatial pattern for the entire body to be examined quantitatively. The body was divided into 9 regions as follows: region 1, head; region 9, foot; the body column was subdivided into 7 regions of equal axial length. Starting at the region just proximal to the head, they are termed regions 2–8 (see Fig. 7). In each region we measured the number of $CC04^+$ neurons and the area of the body on the half of the animal facing the objective. We calculated the density from the number of $CC04^+$ neurons per unit area. We used the value of 4.68×10^{-2} mm^2 as the unit area (which was the frame size of the photomicrograph) because we could then directly use the number of neurons in the frame as the density.

RESULTS

Staining specificity of CC04 antibody

The monoclonal antibody CC04 was originally characterized by indirect immunofluorescence on whole-mount preparations as binding to some interstitial cells in the oogenesis pathway and to the endoderm in *Pelmatohydra robsta*. When assayed on whole-mounts of *Hydra viridissima*, CC04 labeled a large number of neurons, nematocytes, and a small number of nematoblasts, but did not stain other cells (Fig. 1A,B). The cell bodies and neurites of the $CC04^+$ neurons could be visualized clearly in whole-mounts and on cells in macerated preparations. The $CC04^+$ neurons are ganglion cells whose cell bodies are located at the base of the ectoderm (Fig. 1C,D). We could easily distinguish the $CC04^+$ neurons from other stained cell types because of the small size of the cell bodies, the presence of the neurites, and the absence of nematocyst capsules.

Spatial distribution of the $CC04^+$ neurons

Two or three neurites protruded from the cell body of each $CC04^+$ neuron, and mainly ran in a proximodistal direction along the body axis (Fig. 2B–H). Tentacles lacked $CC04^+$ neurons, and there were very few $CC04^+$ neurons in the hypostome (Fig. 2A,B). $CC04^+$ neurons were fairly uniformly distributed along the entire length of the body column although there was some local variation. $CC04^+$ neurons were observed in all parts of the gastric region (Fig. 2C-F), peduncle (Fig. 2G), and in the foot (Fig. 2H). Figure 3 shows the overall distribution of $CC04^+$ neurons in *H. viridissima*. The density of $CC04^+$ nerves is high in the basal disk, with the density decreasing in the peduncle to a level identical to that in the gastric region.

Binding of anti-vasopressin antiserum to the neurons of *H. viridissima*

Neurons showing vasopressin-like immunoreactivity (VLI) have been observed in other species of Hydra (Grimmelikhuijzen et al., 1982a; Koizumi and Bode, 1991; Koizumi, unpublished results). We examined whether there are VLI^+ neurons in *H. viridissima*. VLI^+ neurites could be clearly visualized in whole-mount preparations (Fig. 4). Although it was difficult to identify the cell bodies confidently in many cases, a small number of VLI^+ nerve cell

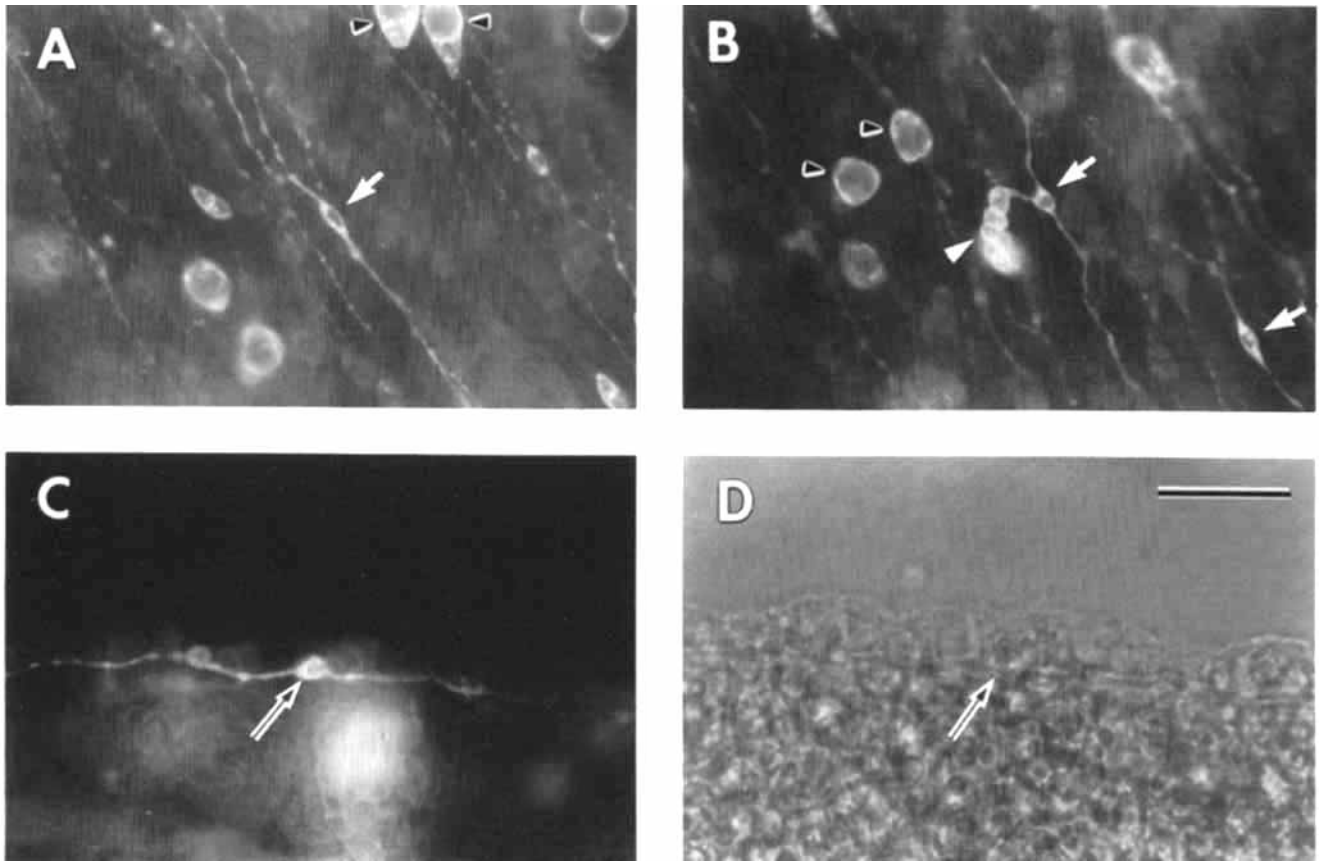

Fig. 1. CC04 staining in the gastric region of *H. viridissima*. **A,B:** The neurons (white arrows), nematocytes (black arrowheads), and a cluster of nematoblasts (a white arrowhead) could be clearly visualized with indirect immunofluorescent in whole-mounts. **C,D:** A tangential view of single CC04$^+$ neuron in fluorescence (C) and in phase contrast (D). Black arrows indicate the same position. Scale bar = 30 μm.

bodies could be recognized in the body column (Fig. 4D,G; arrowheads). In those cases, it was possible to identify the cells as ganglion cells which had two or three neurites. Moreover, double labeling studies revealed that all of the CC04$^+$ neurites for which corresponding cell bodies were evident were VLI$^+$, and that the CC04$^+$ cell bodies were also VLI$^+$ (Fig. 5 and Table 1; see below). When we did immunocytochemical analyses in other species of Hydra (*H. oligactis* and *H. magnipapillata*), the spatial pattern of the VLI$^+$ nerve net which was recognized by the antiserum we used was the same as the results previously reported by others (data not shown). Thus, we concluded that the VLI$^+$ structures that we are seeing in *H. viridissima* are nerve cell processes.

Spatial distribution of the VLI$^+$ nerve net

We found that the VLI$^+$ nerve net extended throughout the entire body of the animal (Fig. 4), with the density of the net being highest in the hypostome (Fig. 4B) and in the foot (Fig. 4H). The VLI$^+$ neurites run primarily in a proximodistal direction in the body column. The density of the VLI$^+$ neurites was uniform along the entire length of the gastric region (Fig. 4C–F). In the peduncle the density of VLI$^+$ neurites is almost the same as in the gastric region (Fig. 4G). Figure 6 shows the overall spatial pattern of the VLI$^+$ nerve net in *H. viridissima*.

The relationship between the CC04$^+$ and the VLI$^+$ nerve nets in the body column

The density of the VLI$^+$ nerve net was higher than that of the CC04$^+$ nerve net in the body column (Figs. 3, 6). To examine the relationship between these two nerve nets, double labeling studies on whole-mount preparations were carried out. The CC04$^+$ neurons in the body column were always VLI$^+$ as well (Fig. 5 and Table 1). On the other hand, about 50% of randomly chosen VLI$^+$ neurites in the body column were CC04$^+$. These results indicate that the CC04$^+$ neuron class is a subset of the VLI$^+$ neuron class.

To determine what percentage of neurons in the gastric region are CC04$^+$, immunocytochemical analysis on cells from macerated preparations was done. The results showed that about 50% of the neurons in the gastric region were CC04$^+$ (Table 2).

Taken together, these data suggest that most of the neurons in the gastric region are VLI$^+$ in this species of hydra. However, because immunostaining for VLI on macerated cells does not work, we could not directly examine this possibility.

Quantitative analysis of CC04$^+$ neuron density

To examine the density of the CC04$^+$ neurons quantitatively, we optically divided the entire body into 9 regions, and calculated the density of CC04$^+$ neurons in each region.

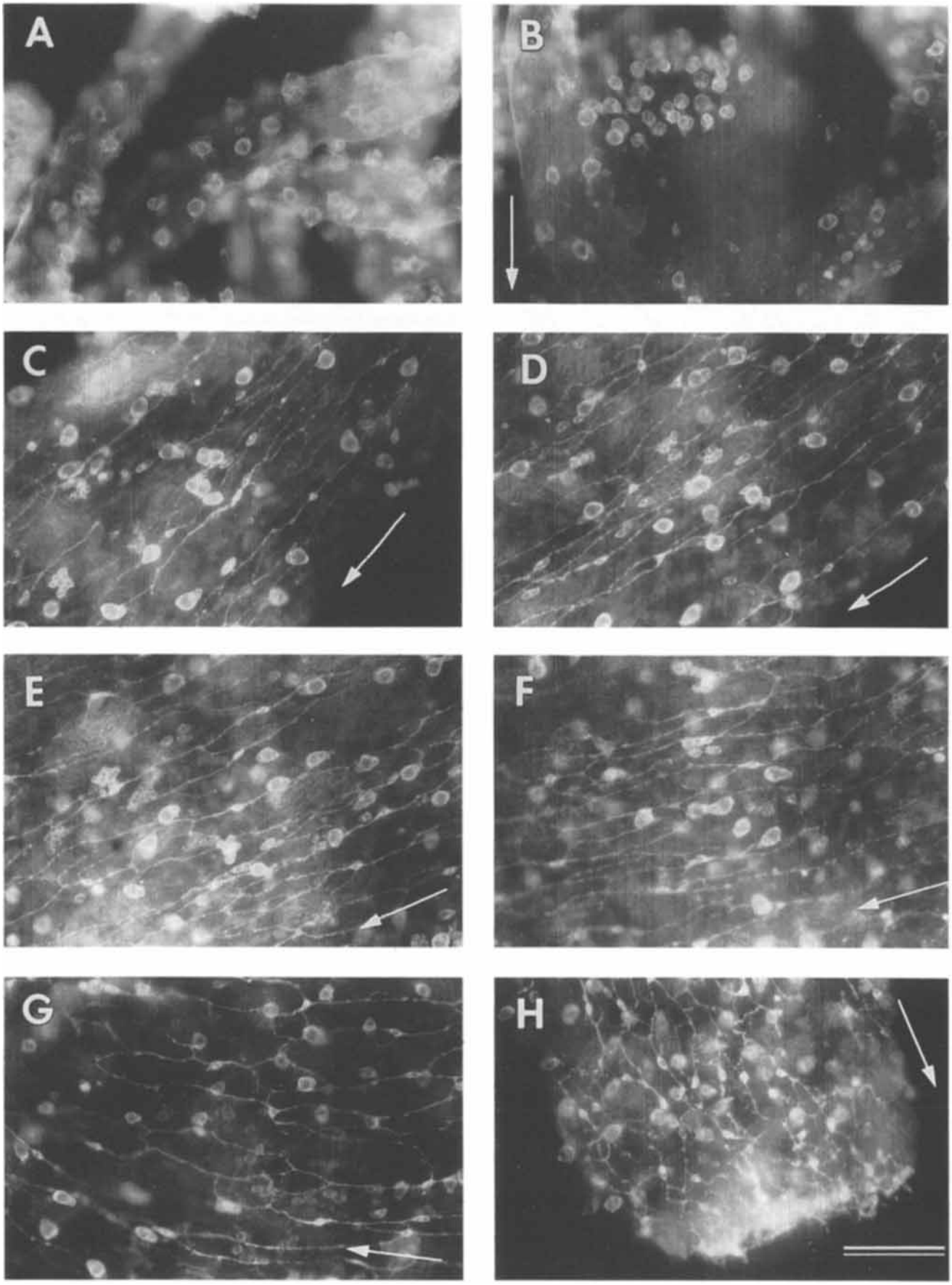

Fig. 2. CC04 staining in different regions of a budless polyp of *H. viridissima:* (**A**) the tentacles, (**B**) the hypostome, (**C**) the upper gastric region, (**D**) the middle gastric region, (**E**) the lower gastric region distal to the budding zone, (**F**) the budding zone, (**G**) the peduncle, and (**H**) the basal disk. Arrows indicate the direction of the body axis (from head to foot). Scale bar = 60 μm.

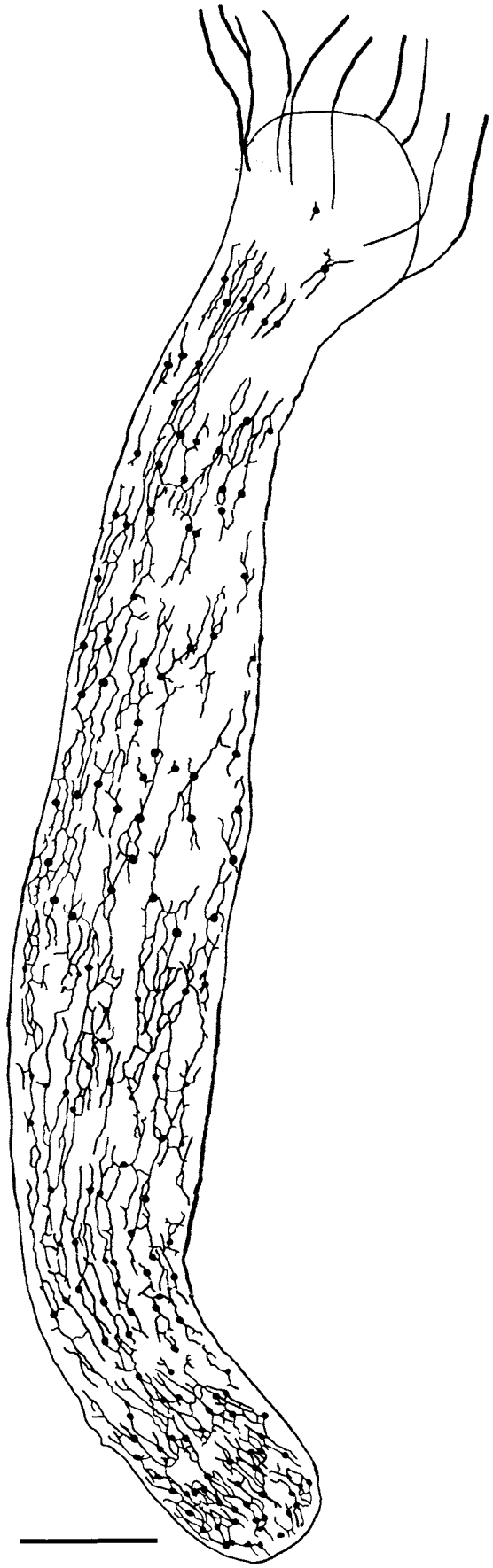

As shown in Figure 7A, the density in each subregion of the gastric region (regions 2–6) showed the same value in the animals which lack a bud. There were very few CC04$^+$ neurons in the head (region 1). In the upper peduncle (region 7), the density was slightly higher than that in the gastric region. The density gradually increased toward the proximal end of the animal. Thus, the density in the lower peduncle (region 8) was 1.5 to 2-fold higher than that in the gastric region. The density in the basal disk (region 9) was 3-fold higher than that in the gastric region. The reason for this increase was a decrease in area and an increase in neuron number in these regions compared with those in the gastric region (Fig. 7B,C). Because of variations in size among individual animals, the neuron number and area in each region fluctuated slightly, resulting in large standard deviations. However, the density in each region is rather constant as shown by a small standard deviation for this measure. These results indicate that the density of CC04$^+$ neurons is maintained at a relatively constant value throughout the gastric region.

Formation of the CC04$^+$ nerve net during asexual development

Hydra multiplys asexually via budding (Otto and Campbell, 1977a). Figure 8 shows the CC04$^+$ nerve net during bud formation. As described above, the neurites of the CC04$^+$ neurons run in a proximodistal direction in the body column of a budless animal (Fig. 8A). When a bud protruded from the parent body, the neurites in the budding zone of the parent lost their polarity (Fig. 8B). The neurites in the parent body became oriented toward the peak of the bud protrusion. In the bud itself, the neurites run in a base to apex direction, which is perpendicular to the parent body axis (Fig. 8D,E). When the basal disk of the bud became obvious, the neurites of the parent body returned to a proximodistal orientation (Fig. 8E). The same features were seen with the VLI$^+$ nerve net in budding animals as with the CC04$^+$ net (not shown).

CC04$^+$ neuron density in the gastric region during asexual development

We examined whether the CC04$^+$ neuron density in the gastric region changes at any stage during asexual development. The density of CC04$^+$ neurons in the lower half of a bud (except for the proximal one-fourth) was analyzed. After the bud was detached from the parent, we referred to the bud as a detached polyp (P), which was then the new parent for the next generation; the neuron density in the budding zone of such animals was then analyzed. As shown in Figure 9, the density of CC04$^+$ neurons was maintained at a constant value at every stage of asexual development. However, the number of the CC04$^+$ neurons in the animal gradually increased during asexual development, reaching a constant level at the later stages. These results show that the CC04$^+$ neuron density in the gastric region is kept constant during asexual development.

CC04$^+$ neuron density during regeneration

We examined whether the CC04$^+$ neuron density in the gastric region changes during foot regeneration. Animals

Fig. 3. The spatial pattern of CC04$^+$ nerve net in *H. viridissima*. The CC04$^+$ neurons were traced on transparent films from the combined photomicrographs. The cell bodies were depicted as single enlarged filled circles to clearly show them. Scale bar = 200 μm.

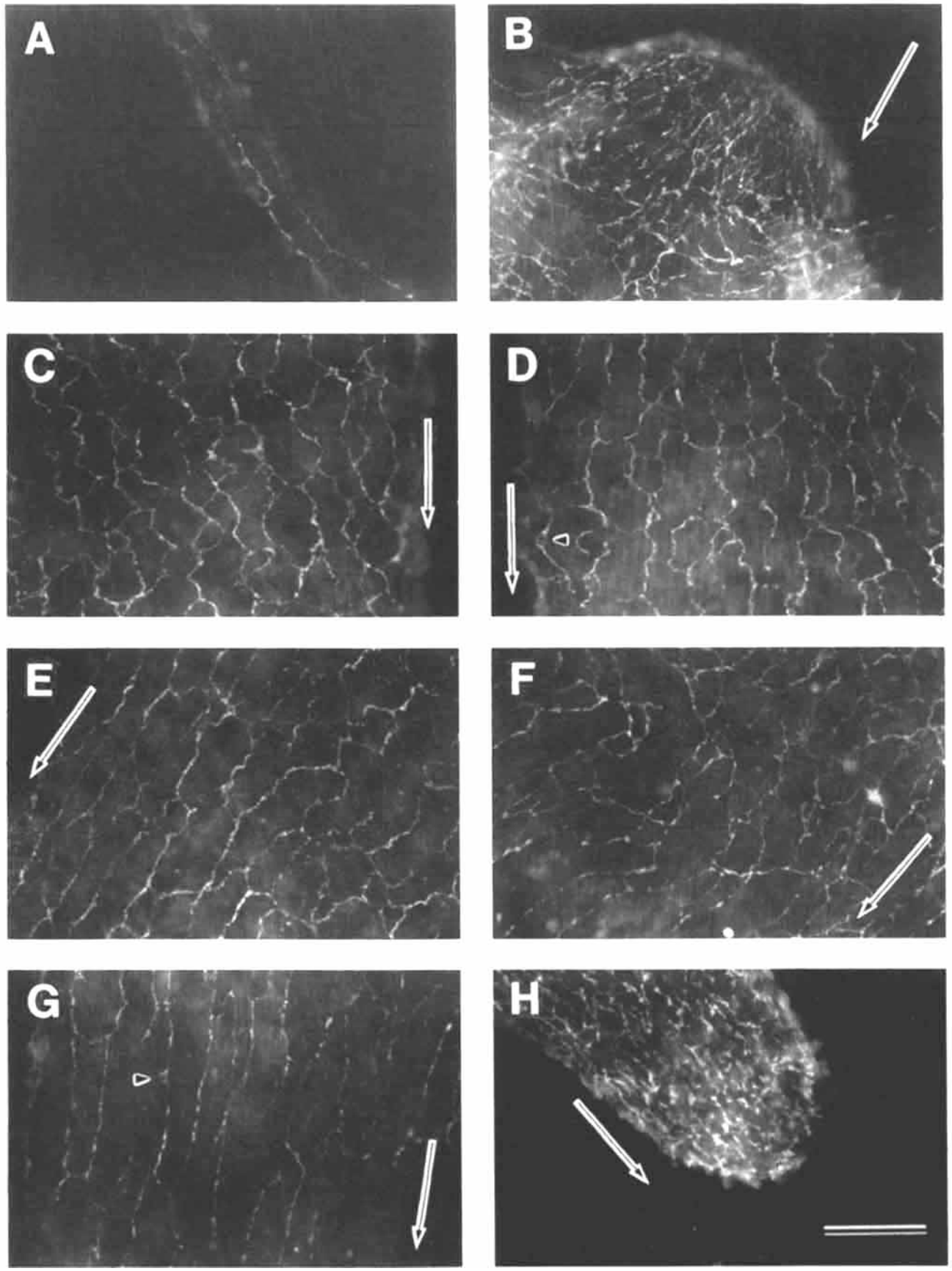

Fig. 4. Anti-vasopressin antiserum staining in different regions of a budless polyp of *H. viridissima:* (**A**) the tentacle, (**B**) the hypostome, (**C**) the upper gastric region, (**D**) the middle gastric region, (**E**) the lower gastric region distal to the budding zone, (**F**) the budding zone, (**G**) the peduncle, and (**H**) the basal disk. The neurite-like structure could be clearly visualized. A small number of the cell bodies could be visualized (D, G; arrowheads). Arrows indicate the direction of the body axis (from head to foot). Scale bar = 60 μm.

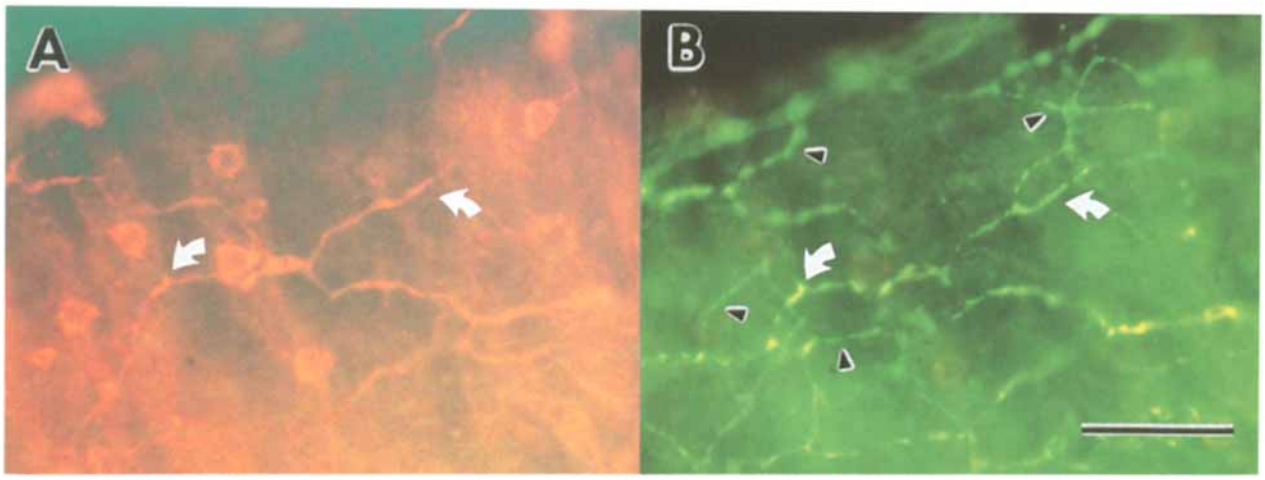

Fig. 5. Double staining in the gastric region of *H. viridissima* with CC04 antibody and anti-vasopressin antiserum. The animal was double-stained with CC04 antibody plus Texas Red-conjugated second antibody (**A**) and anti-vasopressin antiserum plus FITC-conjugated second antibody (**B**). White arrows indicate double stained neurites. Black arrowheads indicate VLI$^+$ neurites which are CC04$^-$. Scale bar = 40 μm.

TABLE 1. Relationship Between CC04$^+$ and VLI$^+$ Nerve Nets in the Body Column of *H. viridissima*[1]

Type	Animals analyzed (n)	Neurites analyzed (n)	Subtype and the number (n)		Fraction of subtype/type (%)
CC04$^+$	20	1820	VLI$^+$	1,820	100
			VLI$^-$	0	0
VLI$^-$	5	954	CC04$^+$	436	45.7
			CC04$^-$	518	54.3

[1]Data were obtained from immunocytochemical analysis on whole-mounts.

without buds were bisected at the midgastric region (Fig. 10A). The distal half of the polyp was allowed to regenerate. Three hours after bisection, the proximal end of the distal half showed the same density of CC04$^+$ neurons as the gastric region (Fig. 10B). One day after bisection, the density in the proximal end was higher than that in the gastric region although there was a large fluctuation in this value. Thereafter the density in the proximal end was maintained at a high level. Foot regeneration was complete 4 to 5 days after bisection. The density of CC04$^+$ neurons in the gastric region of the regenerate showed a constant value during regeneration. These results show that the CC04$^+$ neuron density is dependent on axial location, and that the CC04$^+$ neuron density in the gastric region is kept constant during regeneration.

Insertion of newly differentiated CC04$^+$ neurons into the preexisting CC04$^+$ nerve net in the body column

Animals were pulse-labeled with BrdU and thereafter double-stained with an anti-BrdU antibody and the CC04 antibody. Figure 11 shows the CC04$^+$ neurons with labeled nuclei in the gastric region 2 days after pulse-labeling. We could identify CC04$^+$ neurons, nematocytes, and nematoblasts by fluorescein labeling and BrdU-positive nuclei by Texas Red labeling. We did, however, also observe nuclei labeled by fluorescein. Since both primary antibodies are mouse IgG and both secondary antibodies are goat anti-mouse IgG, these fluorescein-labeled nuclei are likely due to binding of the fluorescein-conjugated secondary antibody with the anti-BrdU primary antibody. This cross-reaction had no effect on the identification of CC04$^+$ neurons.

We qualitatively examined the presence of the new neurons in the middle gastric region, the lower gastric region distal to the budding zone, and the budding zone as well as in the peduncle and the basal disk. BrdU-labeled CC04$^+$ neurons were observed in the gastric regions 1 day after pulse-labeling. The labeled neurons were scattered in the gastric region. New neurons emerged in locations where there was no preexisting CC04$^+$ neurons. In the peduncle and the basal disk, BrdU-labeled CC04$^+$ neurons were observed 2 days after pulse-labeling. They were also scattered in these regions. These results show that new neurons are inserted at scattered sites in the body column, and that there is apparently no defined zone for insertion of the new neurons in the body column. This question remains to be examined for neurons in the upper gastric region.

DISCUSSION

Structure of the nerve net in the body column

The structure of the nerve net in hydra has been studied using methylene blue staining at first, and thereafter extensively investigated using antibodies which are specific for neurons. Several antibodies that recognize the nerve net in the body column have been reported. Yaross et al. (1986) reported a monoclonal antibody, termed RC9, which bound to a subset of ganglion cells in *H. oligactis*. In the gastric region, RC9 stained ganglion cells as well as interstitial cells and nests of cells in the nematocyte pathway. Koizumi et al. (1988) reported the monoclonal antibody TS26, which bound to a subset of ganglion cells in *H. attenuata*. In the body column, TS26 bound to ganglion cells, interstitial cells, nematoblasts, and nematocytes. However, the spatial pattern of the nerve net in the entire body column in hydra has not been described in detail. Thus, the overall structure, development, and maintenance of the nerve net in the body column is poorly understood. By using a monoclonal antibody, termed CC04, and an antiserum against vasopressin, we could characterize the nerve net in the entire body column of *H. viridissima* in detail.

The CC04 antibody bound to a subset of ganglion cells in the body column. Immunocytochemical analysis on macer-

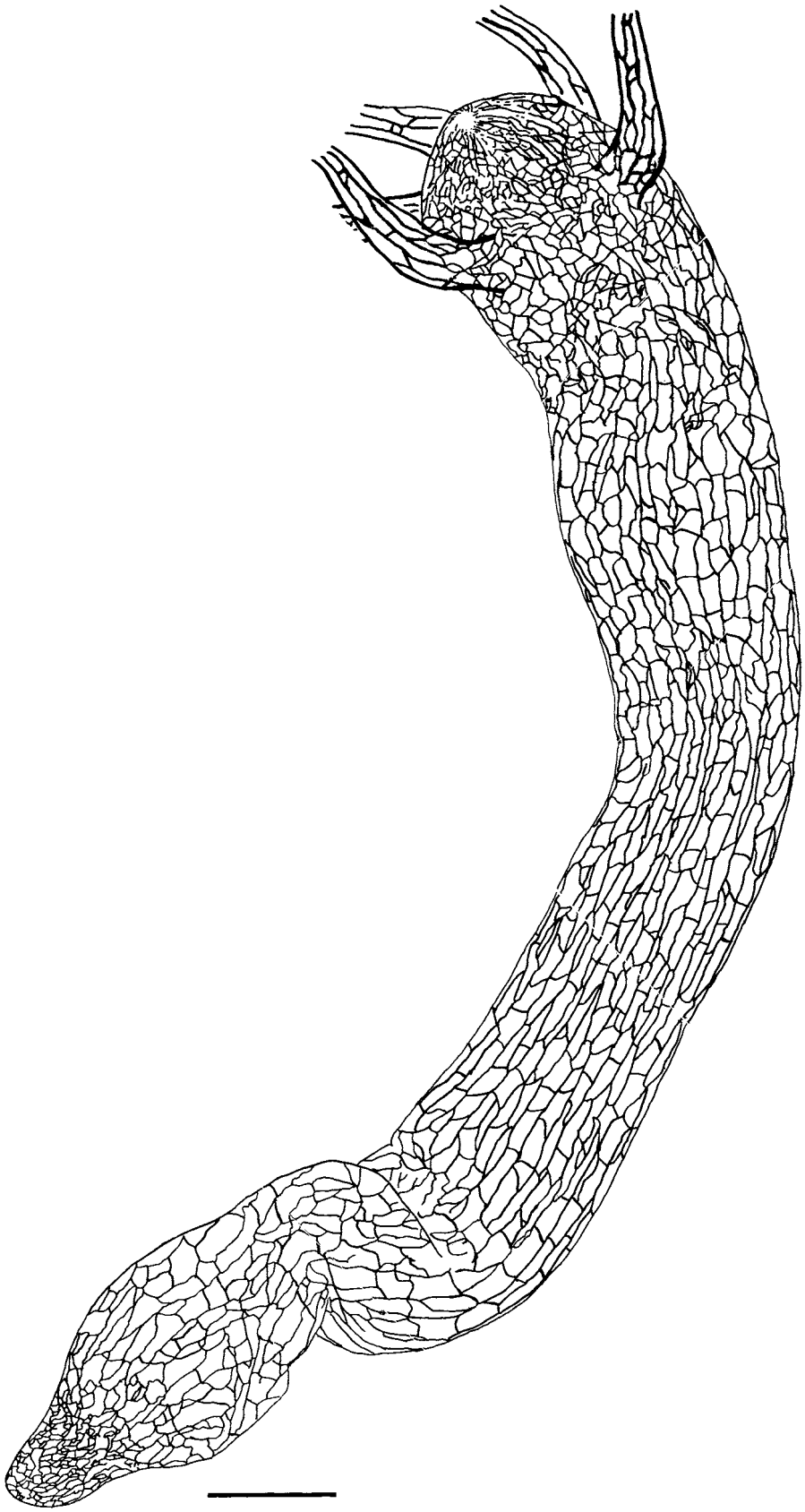

Fig. 6. The spatial pattern of VLI$^+$ nerve net in *H. viridissima*. The nerve net was traced on transparent films from the combined photomicrographs. Scale bar = 200 μm.

TABLE 2. Cell Composition of the Gastric Region of *H. viridissima*[1,2,3]

Cell type	Number (n)	Fraction/ total neurons (%)	Fraction/ ectodermal epitheliomuscular cells (%)
Neurons			
CC04$^+$	53.4 ± 8.0	53.6 ± 0.9	7.2 ± 1.2
CC04$^-$	46.2 ± 8.6		
Total	99.6 ± 16.6		15.6 ± 2.4
Ectodermal epitheliomuscular cells	636 ± 15.5		

[1]Data were obtained from immunocytochemical analysis on macerated cells.
[2]Values shown are mean ± S.D. of five experiments.
[3]No correction was made for the possible loss of macerated cells during the immunocytochemical procedure.

ated preparations showed that half of the neurons in the gastric region were CC04$^+$ (Table 2). The absolute number of each cell type in Table 2 may be an underestimate because some cells may be lost from the glass during preparation. In fact, the number of CC04$^+$ neurons was less than half of that estimated from the immunocytochemical analysis on whole-mount preparations. However, it is unlikely that CC04$^+$ neurons are lost preferentially. It would be expected that all neurons should be lost to the same degree. Therefore no correction was made for the possible loss of macerated cells during the experimental procedure because we were interested in the ratio of CC04$^+$ neurons to total neurons.

Anti-vasopressin (see Figs. 4, 5) antiserum bound to the neurites of neurons, whereas it was difficult to identify the cell bodies in many cases. The VLI$^+$ nerve net extended throughout body of the animal including the body column. In the peduncle, where the tissue is more transparent than in other regions, we could recognize the cell border of ectodermal epitheliomuscular cells in phase contrast of whole-mount specimens in some cases. The size of each ectodermal epitheliomuscular cell in the peduncle seemed to be fairly constant in whole-mount specimens. The area of a mesh of the VLI$^+$ nerve net in the peduncle corresponded to the area occupied by 2 to 3 ectodermal epitheliomuscular cells. These results indicate that the VLI$^+$ nerve net is extensively distributed throughout the body column as well as in the head and the foot.

Double labeling studies on whole-mount preparations revealed that two types of neurons in the body column were defined, CC04$^+$/VLI$^+$ neurons and CC04$^-$/VLI$^+$ neurons. There were no CC04$^+$/VLI$^-$ neurons in the body column. We could not examine whether there are CC04$^-$/VLI$^-$ neurons in the body column. When the VLI$^+$ neuron cell body could be visualized, two or three neurites extended from the cell body in all cases. That is the case for CC04$^+$ neurons. About 50% of the VLI$^+$ neurites which were randomly chosen in the body column were CC04$^+$. As described above, quantitative immunocytochemical analysis on macerated specimens showed that about 50% of neurons in the gastric region were CC04$^+$. These results suggest that most of the neurons in the gastric region are VLI$^+$ in this species of hydra.

In other species of hydra (*H. oligactis, H. magnipapillata,* and *H. vulgaris*), VLI$^+$ neurons are found in the head, in the foot, and in the lower peduncle. Only very small numbers of VLI$^+$ neurons are found in the rest of the body column (Grimmelikhuijzen et al., 1982a; Koizumi and Bode, 1991; Koizumi, unpublished results). We obtained the same results in *H. oligactis* and *H. magnipapillata* using our antiserum (not shown). It is known that the distribution pattern of FMRFamide-like and/or RFamide-

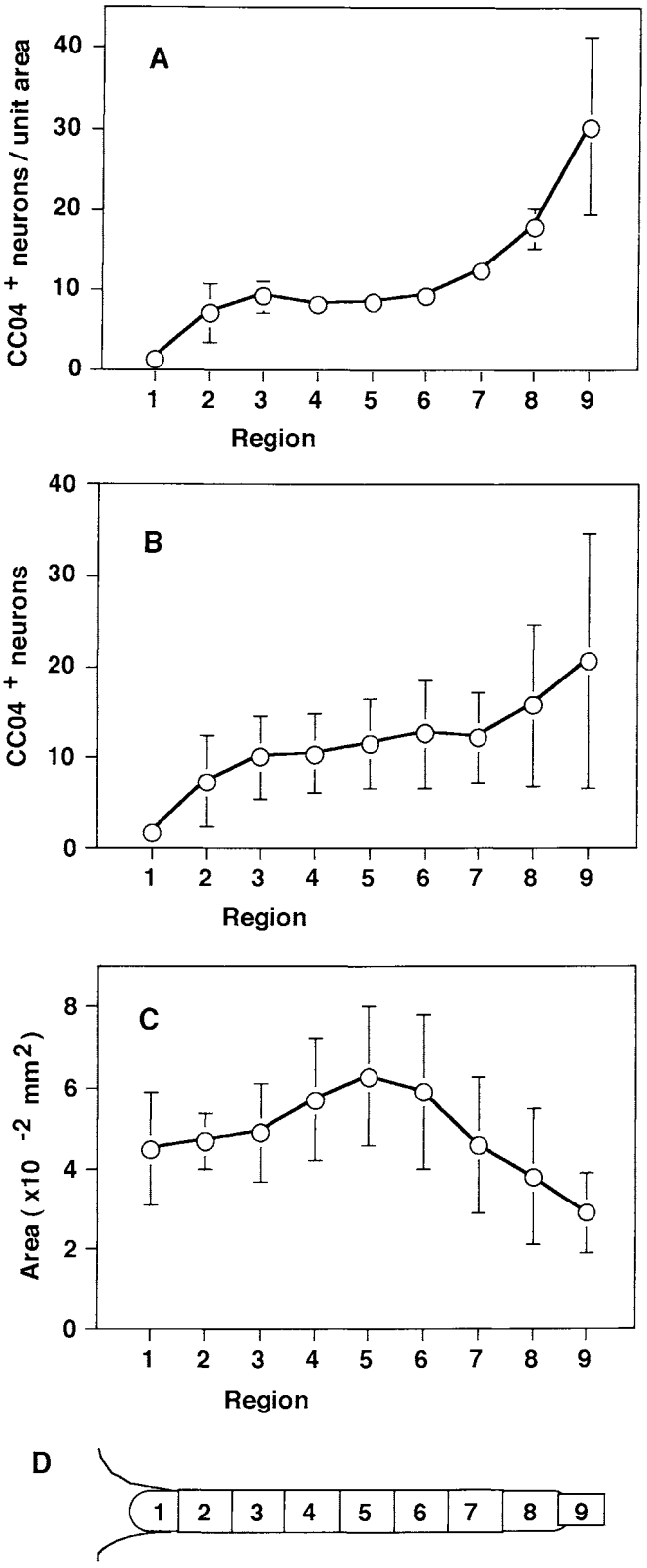

Fig. 7. The CC04$^+$ neuron density in different regions of the budless polyp of *H. viridissima*. **A:** The CC04$^+$ neuron density defined by the number of the neurons per unit area. Unit area = 4.68×10^{-2} mm^2. **B:** The number of CC04$^+$ neurons in each region. **C:** The area in each region. **D:** Schematic representation of each region in a budless polyp. See text for explanation. Each point is the mean of five experiments with standard deviation (S.D.).

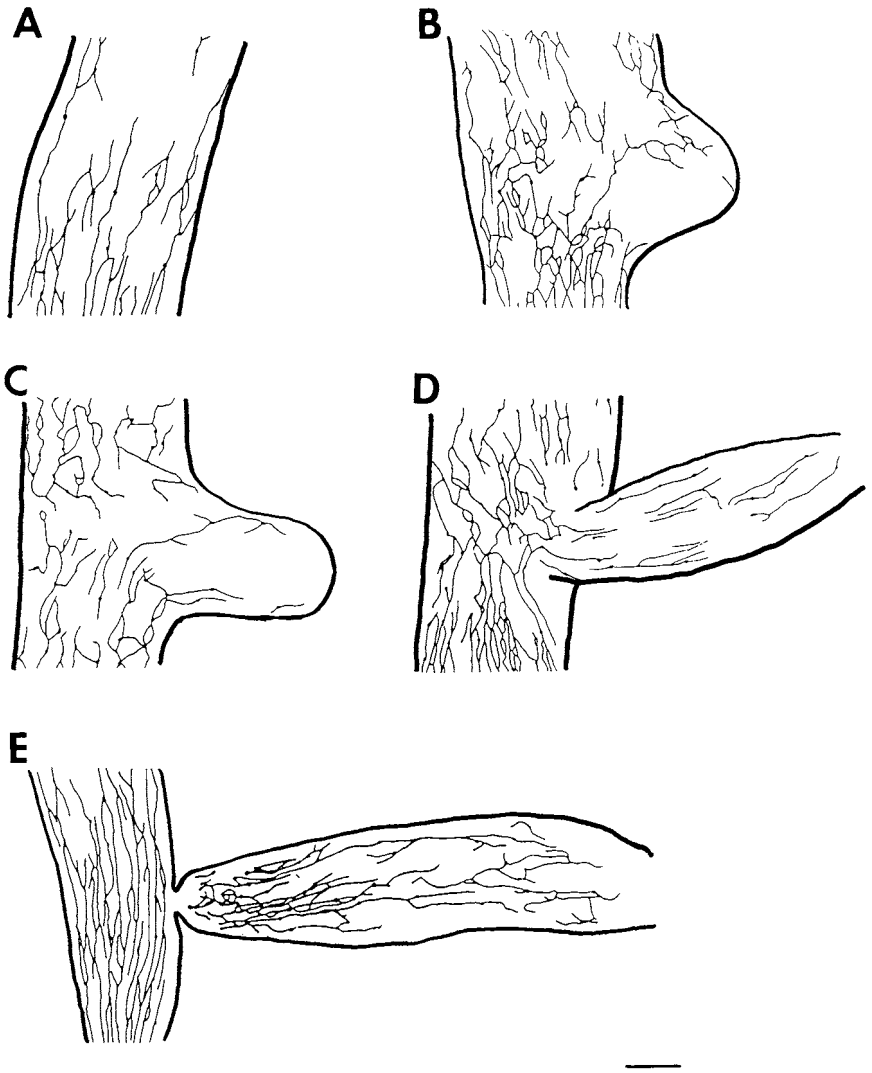

Fig. 8. The spatial pattern of CC04$^+$ nerve net during asexual development (budding) in *H. viridissima:* (**A**) before bud protrusion, (**B**) stage 3, (**C**) stage 5, (**D**) stage 7, and (**E**) stage 9. A bud protrusion is located on the right, whereas the parent is on the left in B–E. Scale bar = 100 μm.

like immunoreactive neurons in *H. oligactis* is similar to that in *H. attenuata,* with two exceptions (Koizumi and Bode, 1986; Koizumi et al., 1992). In both species, the immunoreactive neurons were located in the tentacles, the hypostome, and the peduncle. The narrow perihypostomal nerve ring near the hypostome-tentacle junction was labeled in *H. oligactis,* but not observed in *H. attenuata.* Additionally, a few stained neurons were scattered throughout the body column in *H. oligactis.* The significance of differences in the spatial patterns of VLI$^+$ nerve net in the body column among hydra species remains to be elucidated.

Constant neuron density in the gastric region

By using the maceration technique, Bode et al. (1973) examined neuron density in three subregions of the gastric region, as well as in other regions of *H. attenuata,* which is much larger in size than *H. viridissima.* They reported that the number of neurons per ectodermal epitheliomuscular cell remained constant in the gastric region. We obtained a similar result in *H. viridissima* (Table 2). The number of total neurons/ectodermal epitheliomuscular cell, and the number of CC04$^+$ neurons/ectodermal epitheliomuscular cell, showed a constant ratio in the gastric region.

We quantified the CC04$^+$ neuron density in five subregions of the gastric region as well as in other regions of *H. viridissima.* The whole-mount procedure provided a more precise quantification than the maceration procedure because it was difficult to amputate and divide the polyp into each region precisely before maceration. The results showed that the density was constant throughout the gastric region. During asexual development (budding), the density of neurons in the gastric region was maintained at a constant value at every stage of a generation in spite of continuous growth. Similarly, the density in the gastric region was constant during foot regeneration. During bud formation, epithelial cell division increases significantly in the evaginating bud (Holstein et al., 1991). These results indicate that the neuron density in the gastric region is regulated in a coordinated fashion with epithelial cell division.

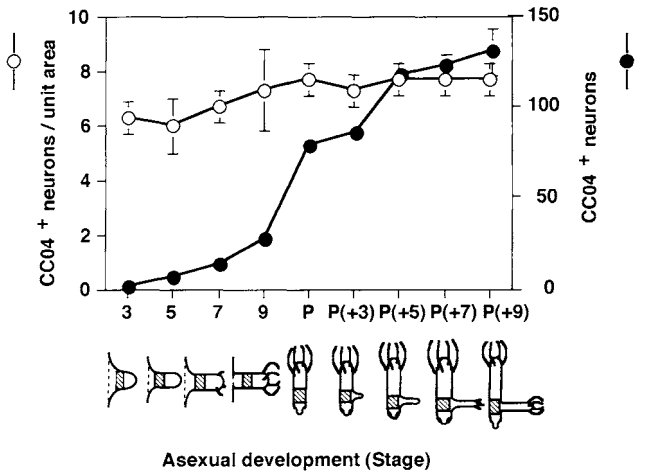

Fig. 9. Quantitative analysis of the CC04$^+$ neurons during asexual development (budding) in *H. viridissima*. The abscissa indicates the stages of development, and the schematic representation: Stages 3–9 (bud stages) are the same as those described for *H. attenuata* by Otto and Campbell (1977a). P represents the dropped polyp. The parentheses represent the stage of a bud (next generation) protruded from the polyp. Open circles indicate the CC04$^+$ neuron density in each stage. The density within the shaded area of the schematic representation was analyzed. See text for explanation. Filled circles indicate the number of CC04$^+$ neurons in the body of each stage of a generation. In the bud stages, the CC04$^+$ neurons in the bud protrusion were counted. In the dropped polyp, the CC04$^+$ neurons in the body except for the bud (the next generation) were counted. Each point is the mean of five experiments with S.D.

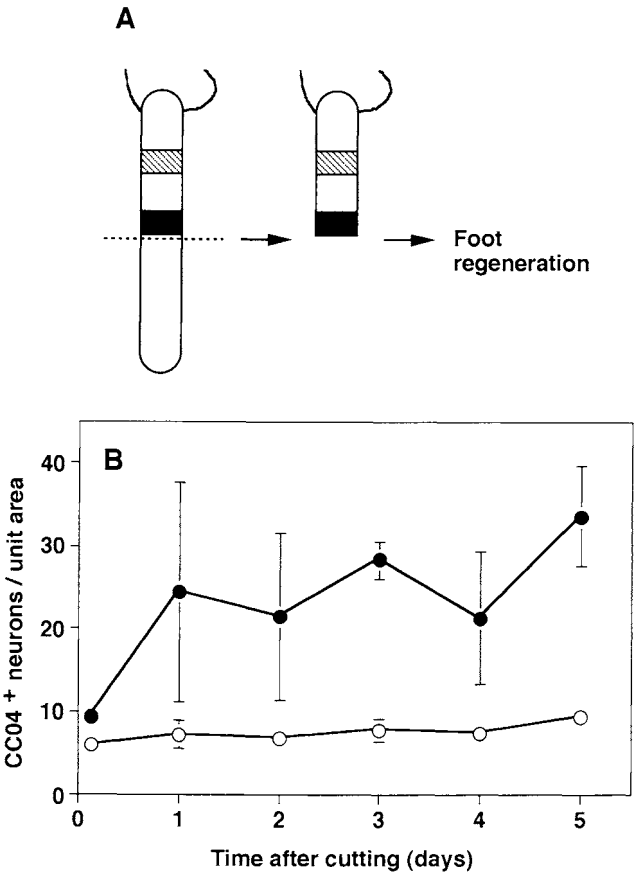

Fig. 10. Effect of foot regeneration on CC04$^+$ neuron density. **A:** The experimental procedure. Budless polyps were bisected in the midgastric region. The distal halves were allowed to regenerate. During the foot regeneration the CC04$^+$ neuron density in the proximal end (black area) and in the gastric region (shaded area) was analyzed. **B:** The CC04$^+$ neuron density during foot regeneration: in the gastric region (open circles), in the proximal end (filled circles). Each point is the mean of five experiments with S.D.

Dependence of neuron density on axial location

The neuron density is sixfold higher in the head, and threefold higher in the foot than in the gastric region (Bode et al., 1973). The density of the VLI$^+$ nerve net was higher in the head and the basal disk than in the gastric region. The CC04$^+$ neuron density was higher in the basal disk than in the gastric region, but there were few CC04$^+$ neurons in the head. During foot regeneration the density of the CC04$^+$ neurons changed in the region which had been the gastric region when this position formed the foot. These results show that neuron density is dependent on axial location.

Insertion of new neurons into the preexisting nerve net in the body column

To elucidate how new neurons are inserted into the preexisting nerve net of the body column, animals were pulse-labeled with BrdU. After pulse-labeling, BrdU-labeled CC04$^+$ neurons appeared in the middle gastric region, the lower gastric region distal to the budding zone, the budding zone, and the peduncle, and the basal disk. We could not examine the appearance of CC04$^+$ neurons in the upper gastric region or in the head. The new neurons were inserted in all regions in a scattered fashion, in agreement with the spatial pattern of epithelial cell division (Holstein et al., 1991). A constant neuron density was thus maintained.

There was some delay (less than 1 day) in appearance of the new neurons in the peduncle and in the basal disk compared to in the gastric region. By continuous labeling with [^{3}H]thymidine and counting each cell type in macerated preparations, David and Gierer (1974) reported that newly differentiated neurons appeared almost simultaneously throughout the body (from hypostome to basal disk) of *H. attenuata*. They also reported that neurons in the peduncle and the basal disk were labeled at a slightly lower rate, in agreement with their observation that the epithelial cells in the peduncle proliferated more slowly than in the gastric region. The reason for the delay we observed is unclear. The delay may be due to time needed for migration of neuron precursors, a final cell division, and differentiation to neurons. Neurons are originally derived from large interstitial stem cells (David and Gierer, 1974; David and Murphy, 1977). Most of the large interstitial cells are located in the gastric region (Bode et al., 1973, 1990). A large interstitial cell committed to neuron differentiation undergoes one or more cell divisions to form small interstitial cells. Small interstitial cells are capable of dividing, and differentiate into neurons (Bode et al., 1990). Neuron precursors migrate along the body column, settle, and complete differentiation (Bode et al., 1988; David and Hager, 1994). It is suggested that neuron precursor migration occurs in S phase of the final cell cycle (David and Hager, 1994). After arrival at the final destination, comple-

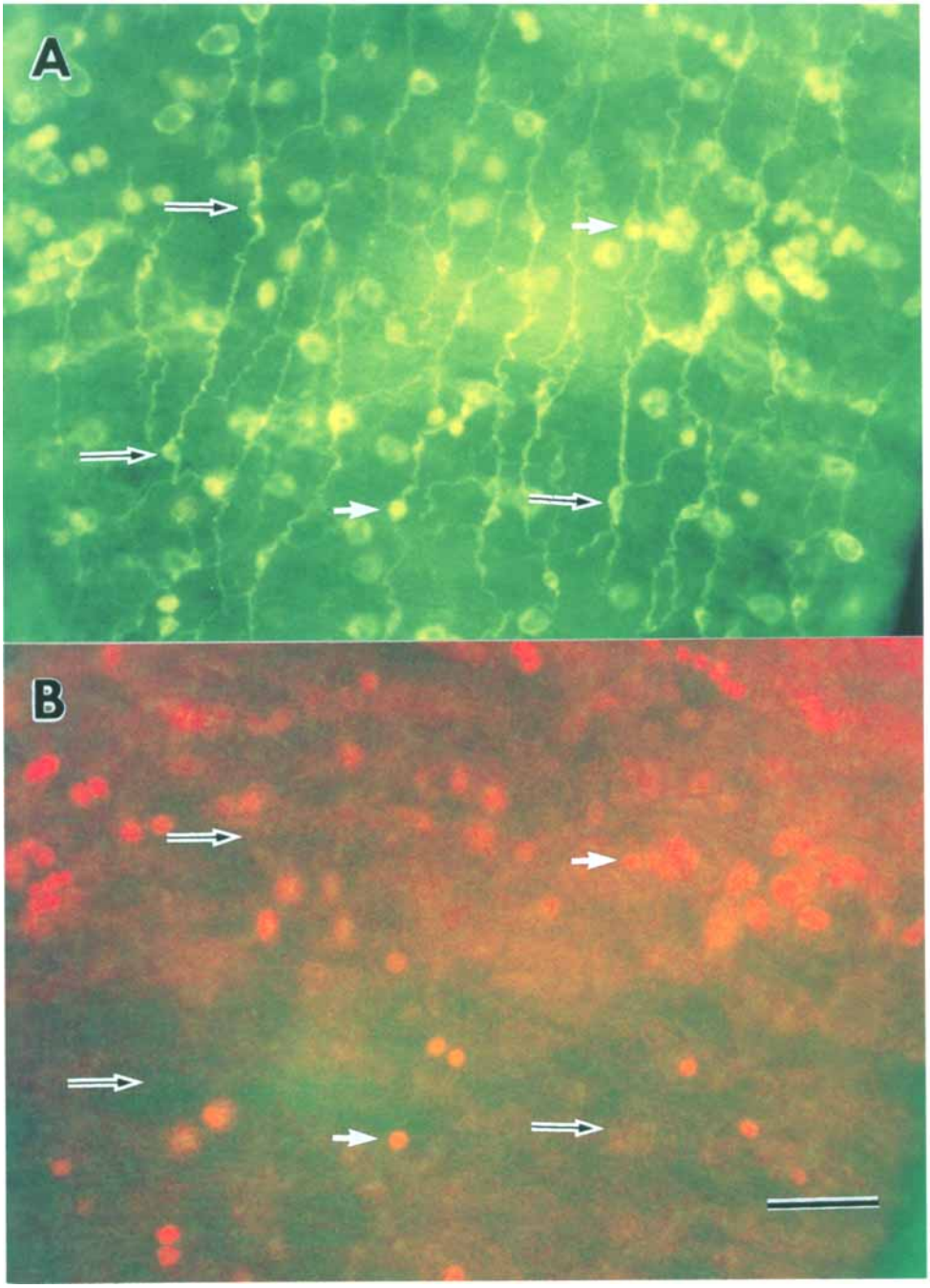

Fig. 11. Double staining of a whole-mount with CC04 and anti-BrdU antibodies in the middle gastric region of the BrdU pulse-labeled animal (2 days after pulse-labeling). A and B were photographed in the same focal plane. **A:** CC04 antibody and FITC-conjugated second antibody staining. **B:** Anti-BrdU antibody and Texas Red-conjugated second antibody staining. White arrows indicate the CC04$^+$ neurons whose nuclei are labeled with BrdU. Black arrows indicate the CC04$^+$ neurons whose nuclei are not labeled with BrdU. See the text for explanation. Scale bar = 30 μm.

tion of the cell cycle occurs, followed by differentiation of both daughter cells into neurons.

In summary, we showed the precise spatial pattern of the nerve net in the entire body column of hydra. It is concluded that the neuron density in the gastric region is maintained at a constant value by insertion of new neurons in the nerve net at a rate in keeping with the rate of epithelial cell division.

ACKNOWLEDGMENTS

We are indebted to Dr. T. Sugiyama for supplying strain 55 of *H. viridissima*. We thank Drs. T. Sugiyama, O. Koizumi, R.A. Marck (Shinshu University), and R.E. Steele (University of California at Irvine) for critically reading the manuscript. We are grateful to Dr. T. Kosaka (Kyushu University) for kindly providing the epifluorescence equip-

ment. And we thank Dr. Littlefield (Tulane University, New Orleans) for kindly providing information about the L9 strain of *H. viridissima*. This work was supported by a research grant from the Ministry of Education, Science, Culture, and Sports of Japan.

LITERATURE CITED

Bode, H.R. (1988) Continuous conversion of neuron phenotype in hydra. Trends Genet. *8:*279–284.

Bode, H.R., S. Berking, C.N. David, A. Gierer, H. Schaller, and E. Trenkner (1973) Quantitative analysis of cell types during growth and morphogenesis in hydra. Wilhelm Roux Arch. EntwMech. Org. *171:*269–285.

Bode, H.R., S. Heimfeld, O. Koizumi, C.L. Littlefield, and M.S. Yaross (1988) Maintenance and regeneration of the nerve net in hydra. Amer. Zool. *28:*1053–1063.

Bode, H.R., L.W. Gee, and M.A. Chow (1990) Neuron differentiation in hydra involves dividing intermediates. Dev. Biol. *139:*231–243.

Burnett, A.L., and N.A. Diehl (1964) The nervous system of *Hydra*. I. Types, distribution and origin of nerve elements. J. Exp. Zool. *157:*217–226.

Campbell, R.D. (1967a) Tissue dynamics of steady state growth in *Hydra littoralis*. I. Patterns of cell division. Dev. Biol. *15:*487–502.

Campbell, R.D. (1967b) Tissue dynamics of steady state growth in *Hydra littoralis*. II. Patterns of tissue movement. J. Morph. *121:*19–28.

Campbell, R.D., and H.R. Bode (1983) Terminology for morphology and cell types. In H.M. Lenhoff (ed): Hydra: Research Methods. New York: Plenum Press, pp. 5–14.

David, C.N. (1973) A quantitative method for maceration of hydra tissue. Wilhelm Roux' Arch. EntwMech. Org. *171:*259–285.

David, C.N., and R.D. Campbell (1972) Cell cycle kinetics and development of *Hydra attenuata*. I. Epithelial cells. J. Cell. Sci. *11:*557–568.

David, C.N., and A. Gierer (1974) Cell cycle kinetics and development of *Hydra attenuata*. III. Nerve and nematocyte differentiation. J. Cell Sci. *16:*359–375.

David, C.N., and G. Hager (1994) Formation of a primitive nervous system: Nerve cell differentiation in the polyp hydra. Perspectives Dev. Neurobiol. *2:*135–140.

David, C.N., and S. Murphy (1977) Characterization of interstitial stem cells in hydra by cloning. Dev. Biol. *58:*372–383.

Dunne, J.F., L.C. Javois, L.W. Huang, and H.R. Bode (1985) A subset of cells in the nerve net of *Hydra oligactis* defined by a monoclonal antibody: Its arrangement and development. Dev. Biol. *109:*41–53.

Grimmelikhuijzen, C.J.P. (1983) Coexistence of neuropeptides in hydra. Neuroscience *4:*837–845.

Grimmelikhuijzen, C.J.P., F. Sundler, and J.F. Rehfeld (1980) Gastrin/CCK-like immunoreactivity in the nervous system of coelenterates. Histochemistry *69:*61–68.

Grimmelikhuijzen, C.J.P., A. Baife, P.C. Emson, D. Powell, and F. Sundler (1981a) Substance P-like immunoreactivity in the nervous system of hydra. Histochemistry *71:*325–333.

Grimmelikhuijzen, C.J.P., R.E. Carraway, A. Rokaeus, and F. Sundler (1981b) Neurotensin-like immunoreactivity in the nervous system of hydra. Histochemistry *72:*199–209.

Grimmelikhuijzen, C.J.P., K. Dierickx, and G.J. Boer (1982a) Oxytocin/vasopressin-like immunoreactivity is present in the nervous system of hydra. Neuroscience *7:*3191–3199.

Grimmelikhuijzen, C.J.P., G.J. Dockray, and L.P.C. Schot (1982b) FMR-Famide-like immunoreactivity in the nervous system of hydra. Histochemistry *73:*499–508.

Grimmelikhuijzen, C.J.P., G.J. Dockray, and N. Yanihara (1981c) Bombesin-like immunoreactivity in the nervous system of hydra. Histochemistry *73:*171–180.

Hadzi, H. (1909) Uber das nervensystem von hydra. Arb. Zool. Inst. Univ. Wien *17:*225–268.

Hobmayer, E., T.W. Holstein, and C.N. David (1990a) Tentacle morphogenesis in hydra. I. The role of head activator. Development *109:*887–895.

Hobmayer, E., T.W. Holstein, and C.N. David (1990b) Tentacle morphogenesis in hydra. II. Formation of a complex between a sensory nerve cell and a battery cell. Development *109:*897–894.

Holstein, T.W., E. Hobmayer, and C.N. David (1991) Pattern of epithelial cell cycling in hydra. Dev. Biol. *148:*602–611.

Koizumi, O., and H.R. Bode (1986) Plasticity in the nervous system of adult hydra. I. The position-dependent expression of FMRFamide-like immunoreactivity. Dev. Biol. *116:*407–421.

Koizumi, O., and H.R. Bode (1991) Plasticity in the nervous system of adult hydra. III. Conversion of neurons to expression of a vasopressin-like immunoreactivity depends on axial location. J. Neurosci. *11:*2011–2020.

Koizumi, O., S. Heimfeld, and H.R. Bode (1988) Plasticity in the nervous system of adult hydra. II. Conversion of ganglion cells of the body column into epidermal sensory cells of the hypostome. Dev. Biol. *129:*358–371.

Koizumi, O., M. Itazawa, H. Mizumoto, S. Minobe, L.C. Javois, C.J.P. Grimmelikhuijzen, and H.R. Bode (1992) Nerve ring of the hypostome in hydra. I. Its structure, development, and maintenance. J. Comp. Neurol. *326:*7–21.

Lentz, T.L., and R. Barrnett (1965) Fine structure of the nervous system of hydra. Amer. Zool. *5:*341–356.

Otto, J.J., and R.D. Campbell (1977a) Budding in *Hydra attenuata:* Bud stages and fate map. J. Exp. Zool. *200:*417–428.

Otto, J.J., and R.D. Campbell (1977b) Tissue economics of hydra: Regulation of cell cycle, animal size and development by controlled feeding rates. J. Cell. Sci. *28:*117–132.

Takano, J., and T. Sugiyama (1983) Genetic analysis of developmental mechanisms in hydra. VIII. Head-activation and head-inhibition potentials of a slow-budding strain (L4). J. Embryol. Exp. Morphol. *78:*141–168.

Teragawa, C.K., and H.R. Bode (1990) Spatial and temporal patterns of interstitial cell migration in *Hydra vulgaris*. Dev. Biol. *138:*63–81.

Westfall, J.A. (1973) Ultrastructural evidence for a granule-containing sensory-motor-interneuron in *Hydra littoralis*. J. Ultrastruct. Res. *42:*268–282.

Westfall, J.A., and J.C. Kinnamon (1978) A second sensory-motor-interneuron with neurosecretory granules in hydra. J. Neurocytol. *7:*365–379.

Yaross, M.S., J. Westerfield, L.C. Javois, and H.R. Bode (1986) Nerve cells in hydra: Monoclonal antibodies identify two lineages with distinct mechanisms for their incorporation into head tissue. Dev. Biol. *114:*225–237.